

Semantic Ensemble Loss and Latent Refinement for High-Fidelity Neural Image Compression

Daxin Li, Yuanchao Bai*, Kai Wang, Junjun Jiang, Xianming Liu
Faculty of Computing, Harbin Institute of Technology
hahalidaxin@stu.hit.edu.cn, yuanchao.bai@hit.edu.cn

Abstract—Recent advancements in neural compression have surpassed traditional codecs in PSNR and MS-SSIM measurements. However, at low bit-rates, these methods can introduce visually displeasing artifacts, such as blurring, color shifting, and texture loss, thereby compromising perceptual quality of images. To address these issues, this study presents an enhanced neural compression method designed for optimal visual fidelity. We have trained our model with a sophisticated semantic ensemble loss, integrating Charbonnier loss, perceptual loss, style loss, and a non-binary adversarial loss, to enhance the perceptual quality of image reconstructions. Additionally, we have implemented a latent refinement process to generate content-aware latent codes. These codes adhere to bit-rate constraints, and prioritize bit allocation to regions of greater importance. Our empirical findings demonstrate that this approach significantly improves the statistical fidelity of neural image compression.

Index Terms—Generative Image Compression, Learned Image Compression

I. INTRODUCTION

Powered by deep learning, Learned Image Compression (LIC) has undergone remarkable progress in recent times, as evidenced by numerous studies [2], [3], [8], [14], [22], [23]. Some cutting-edge learning-based approaches now outperform traditional codecs like VVC [4], marking a promising future for LIC technologies. However, a notable challenge arises when these models, optimized for Mean Squared Error (MSE) metrics, produce unsatisfactory visual artifacts at lower bitrates. These artifacts, manifesting as blur and lost textures, result from a misalignment between the optimization objectives and the complexities of human visual perception. Additionally, human observers tend to focus on regions of higher salience or relevance in an image, such as faces, distinct objects, or text, while overlook less critical backgrounds or blurred sections. Thus, uniform bit allocation across an image can adversely affect the perceptual quality of salient areas, especially under limited bandwidth.

Previous methods have addressed image compression challenges by incorporating perceptual and adversarial losses [1], [7], [9], [15], [17]. In this work, we enhance the statistical fidelity of reconstructed images by proposing a semantic ensemble loss and latent refinement. The contributions are summarized as follows:

- We propose a semantic ensemble loss that includes Charbonnier loss, perceptual loss, style loss, and a non-binary adversarial loss. This loss function enables the model to generate more detailed and content-rich images with higher fidelity.
- We refine the latent representations using semantic ensemble loss coupled with stochastic Gumbel annealing. This process can extract latent codes that comply with bit-rate constraints, and allocate more bits to salient image regions.
- Extensive experiments demonstrate that our codec achieves superior perceptual quality compared to existing methods, as evaluated on the CLIC 2024 validation dataset.

II. METHOD

A. Architecture

The overview of our framework is shown in Fig. 1. Our methodology follows the architecture established by HiFiC [17], which includes analysis, synthesis, hyper-analysis, and hyper-synthesis transforms. To improve entropy prediction and efficiency, we incorporate the efficient spatial-channel context model from ELIC [8]. This model segments the latent representations into 10 groups and applies autoregressive prediction to each group.

B. Training with Semantic Ensemble Loss

We train a lossy compression model guided by a rate-distortion loss function, a methodology validated as effective by [9], [17], [18], and articulated as:

$$\mathcal{L} = \lambda^* \mathcal{R} + \mathcal{D} \quad (1)$$

Here, \mathcal{R} and \mathcal{D} represent the rate and distortion contributions, respectively. The hyper-parameter λ^* modulates the balance between these losses, imposing a penalty on the rate if it exceeds the target rate τ :

$$\lambda^* = \begin{cases} \lambda_a, & \text{if } \mathcal{R}^* \leq \tau \\ \lambda_b, & \text{otherwise} \end{cases}, \text{ with } \lambda_b \gg \lambda_a. \quad (2)$$

Note that \mathcal{R}^* is the actual rate, derived from the quantized latents, whereas \mathcal{R} is computed from the noised latents to enable differentiability. The distortion is quantified using our proposed semantic ensemble loss that

* Corresponding Author: Yuanchao Bai

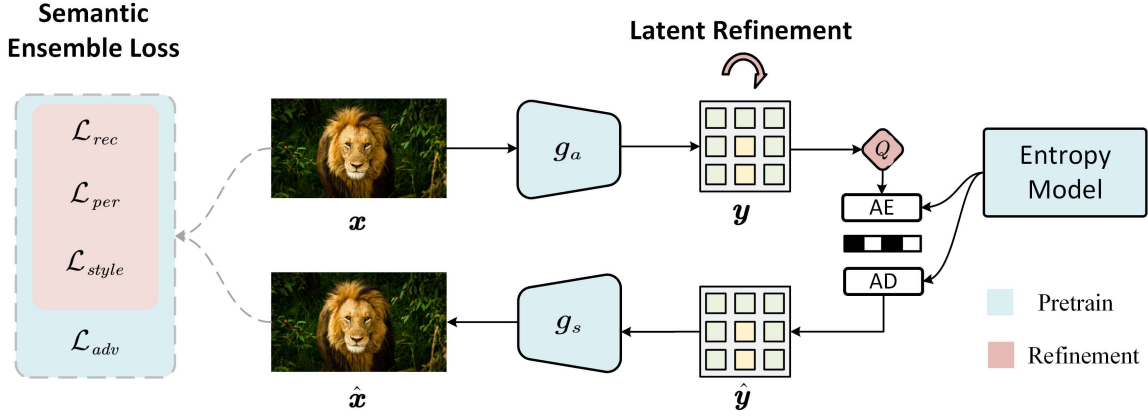


Fig. 1: Framework Overview: Our process begins with training a VAE-based compression model employing our semantic ensemble loss, which is subsequently refined using SGA and a computationally simplified loss.

incorporates reconstruction, perceptual, style, and adversarial losses:

$$\mathcal{D} = \alpha \mathcal{L}_{\text{rec}} + \beta \mathcal{L}_{\text{per}} + \gamma \mathcal{L}_{\text{style}} + \delta \mathcal{L}_{\text{adv}}. \quad (3)$$

In this equation, α , β , γ , and δ are hyper-parameters that balance the four respective loss components. The reconstruction loss, \mathcal{L}_{rec} , employs the Charbonnier loss [13] to measure fidelity between the original and reconstructed images. The perceptual loss [25], \mathcal{L}_{per} , is derived from the L_2 loss between feature representations extracted by VGG of the original and reconstructed images. The style loss [9], [20], $\mathcal{L}_{\text{style}}$, calculates the L_2 loss between the Gram matrices of 16×16 feature patches from the original and reconstructed images, emphasizing differences in local textures. Lastly, the adversarial loss, \mathcal{L}_{adv} , is associated with the discriminator’s loss.

To further enhance the visual quality of the reconstructed images, we have integrated a non-binary adversarial discriminator within the Vector Quantized-Variational AutoEncoder (VQ-VAE) framework, following the approach by Muckley *et al.* [18]. This discriminator significantly improves the decoder’s ability to distinguish between real and reconstructed images, focusing on capturing differences at a more refined semantic level. The adversarial loss associated with this discriminator is expressed as:

$$\begin{aligned} \mathcal{L}_{\text{disc}}(\phi) &= \mathbb{E}_{\mathbf{x} \sim P_{\mathbf{X}}} [-\langle \mathbf{u}(\mathbf{x}), \log D_{\phi}(\mathbf{x}) \rangle] \\ &\quad + \mathbb{E}_{\hat{\mathbf{x}} \sim P_{\hat{\mathbf{X}}}} [-\langle \mathbf{b}_0, \log D_{\phi}(\hat{\mathbf{x}}) \rangle], \\ \mathcal{L}_{\text{adv}}(\varphi, \omega, \mathbf{v}) &= \mathbb{E}_{\hat{\mathbf{x}} \sim P_{\hat{\mathbf{X}}}} [-\langle \mathbf{u}(\mathbf{x}), \log D_{\phi}(\hat{\mathbf{x}}) \rangle], \end{aligned} \quad (4)$$

where D_{ϕ} , the discriminator, is parameterized by ϕ . Here, $\mathbf{u}(\mathbf{x})$ is a one-hot vector corresponding to the index of the nearest neighbor in the codebook, and \mathbf{b}_0 denotes the absence of such a neighbor (the ‘fake’ label). The parameters φ , ω , and \mathbf{v} represent the encoder, the entropy model, and the decoder, respectively.

C. Latent Refinement for Perception

To enhance alignment with the original image content, we apply semi-amortized optimization to derive content-adaptive latent representations. Drawing on the methods of Yang *et al.* [24] and Gao *et al.* [6], we employ Stochastic Gumbel Annealing (SGA) to generate the modified latent variable, and retrieve the dequantized latent representation $\tilde{\mathbf{y}}$ through a learnable process as described in Gao *et al.* [6]:

$$\tilde{\mathbf{y}} = \text{SGA}(\mathbf{y}/\Delta)\Delta, \quad (5)$$

where Δ is the learnable quantization step. For hyper latent variable z , we only use SGA without learnable quantization to derive \bar{z} . We manage the bitrate with a rate-constrained loss, including a simplified semantic ensemble loss as distortion, defined as follows:

$$\begin{aligned} \mathcal{L}(\mathbf{y}, \mathbf{z}) &= \lambda^* \cdot \mathcal{R} + \mathcal{D} \\ &= -\lambda^* \cdot (\log p_{\omega}(\tilde{\mathbf{y}}; \bar{\mathbf{z}}) + \log p_{\omega}(\bar{\mathbf{z}})) \\ &\quad + \alpha \mathcal{L}_{\text{rec}} + \beta \mathcal{L}_{\text{per}} + \gamma \mathcal{L}_{\text{style}}, \end{aligned} \quad (6)$$

where λ^* , derived from Eq. 2, ensures the bitrate aligns with the target. The hyperparameters α , β , and γ balance the trade-off between distortion and fidelity. The adversarial loss is excluded due to its intensive computation. Furthermore, as demonstrated in Gao *et al.* [6], by refining the latent representations, we can redistribute bits to prioritize more significant regions. Specifically, we compute distortion losses for foreground and background regions separately, leveraging image-wise calculations for perceptual and style losses. This process is encapsulated by:

$$\mathcal{D}_{\text{roi}} = \lambda_{\text{fg}} \cdot \mathbf{m} \odot \mathcal{D}_{\text{fg}} + \lambda_{\text{bg}} \cdot (1 - \mathbf{m}) \odot \mathcal{D}_{\text{bg}}, \quad (7)$$

where \mathbf{m} denotes the foreground mask. The hyperparameters λ_{fg} and λ_{bg} balance the foreground and background losses, \mathcal{D}_{fg} and \mathcal{D}_{bg} , respectively, which include similar terms to those in Eq. 6. To obtain a dedicated

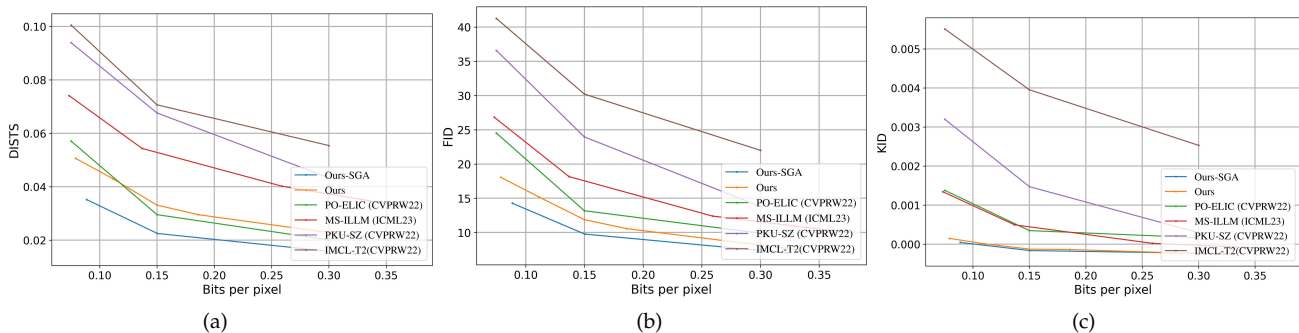


Fig. 2: Comparisons of methods across various distortion and statistical fidelity metrics for the CLIC 2024 validation set.

mask for refining the latent representations, we utilize label tools¹ assisted by Segment Anything (SAM) [11]. SAM conveniently accepts mouse points as input and generates a corresponding mask with finer edges, as illustrated in Fig. 4.

III. EXPERIMENTS

A. Settings

Our model is trained using 256×256 patches extracted from the test split of the OpenImages V7 dataset [12]. We employ the AdamW optimizer with parameters $\beta_1 = 0.9$ and $\beta_2 = 0.999$, conducting the training over 2 million iterations. Our training methodology is in line with that of Muckley *et al.* [18], which involves a two-stage process for generative models. Initially, we perform end-to-end training with a rate-constrained loss function, optimizing both rate and distortion losses, including reconstruction, perceptual, and style loss components. This is followed by a fine-tuning stage of the decoder to incorporate an adversarial loss using a non-binary discriminator. The hyperparameters in Eq. 3 are experimentally set to $\alpha = 10$, $\beta = 1$, $\gamma = 80$, $\delta = 0.008$ respectively during training.

For benchmarking, we compare our results with several state-of-the-art models, including MS-ILLM [18], and leading entries from the CLIC2022 challenge, such as PO-ELIC [9], PKU-SZ [16], and IMCL-T2 [19]. We obtain reconstructed images from the official CLIC2022 challenge website and calculate metrics following the methodology described in Muckley *et al.* [18]. For evaluation, we use the validation set of CLIC2024 (test set of CLIC2022), comprising 30 high-resolution 2k images. Performance is assessed using reference metrics—such as DISTs [5] (better than PSNR, MS-SSIM in measuring visual consistency)—and non-reference metrics, including FID [10] and KID [21].

B. Main Performance

Our method exhibits superior performance in FID and KID metrics, outshining all compared methodologies as

referenced in MS-ILLM [18], PO-ELIC [9], PKU-SZ [16], and IMCL-T2 [19]. In the DISTs metric, it matches the top performance of PO-ELIC [9]. Specifically, our approach surpasses the former state-of-the-art, MS-ILLM [18], with a remarkable 42.49% BD-Rate reduction in the FID metric, a 58.87% reduction in the KID metric, and a 53.00% reduction in the DISTs metric. The Ours-SGA variant of our method, which further refines latent representations, notably enhances both statistical fidelity and textural details. Consequently, Ours-SGA achieves the highest scores across FID, KID, and DISTs metrics. Remarkably, in comparison with MS-ILLM [18], Ours-SGA attains a more substantial BD-Rate reduction of 62.00% in the FID metric, 67.06% in the KID metric, and a significant 74.63% in the DISTs metric, underscoring our methodology’s effectiveness in producing images of superior perceptual quality.

C. Qualitative Results

As shown in Fig. 3, at the same bitrate, visual comparisons of the compression and reconstruction images using different methods demonstrate that our approach excels in generating details and maintaining consistency with the original image. Specifically, it outperforms POELIC and MS-ILLM in preserving finer details, such as the texture around the lion’s eye and the leaf’s structure, achieving higher fidelity to the original content.

Fig. 4 displays visual results that validate the effectiveness of ROI-based latent refinement. The left two images show the original image and its corresponding mask. For comparison, we include results from L_0 training without ROI-based loss and from methods L_1 and L_2 , employing ROI-based loss with different weights $\lambda_{fg} = (1, 1)$ and $\lambda_{bg} = (0, 0.2)$. ROI-based loss enhances fidelity and texture details in the foreground, while training focused solely on ROI distortion leads to noticeable artifacts, as seen in L_2 . The distinct weighting of foreground and background in L_1 yields optimal performance, enhancing foreground quality while preserving background regions, demonstrating our method’s efficacy in bit allocation to enhance perceptual quality.

¹<https://github.com/anuragxel/salt>

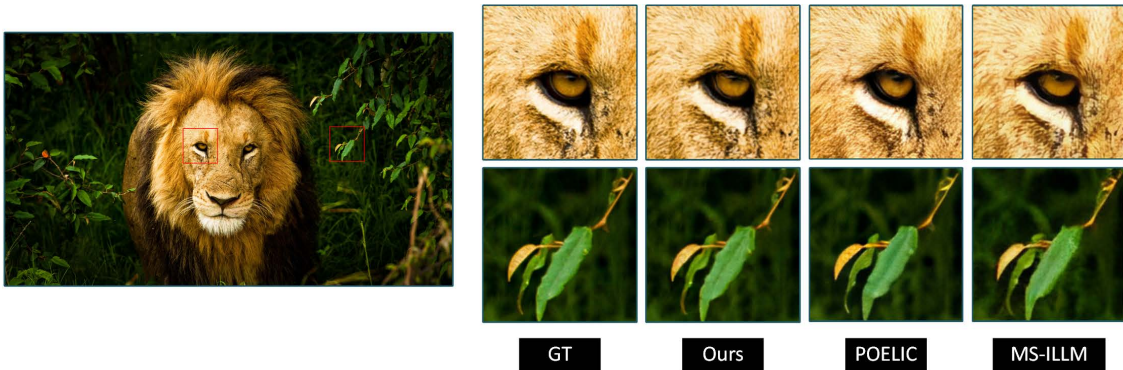


Fig. 3: Visual comparisons using different methods at the same bitrate.

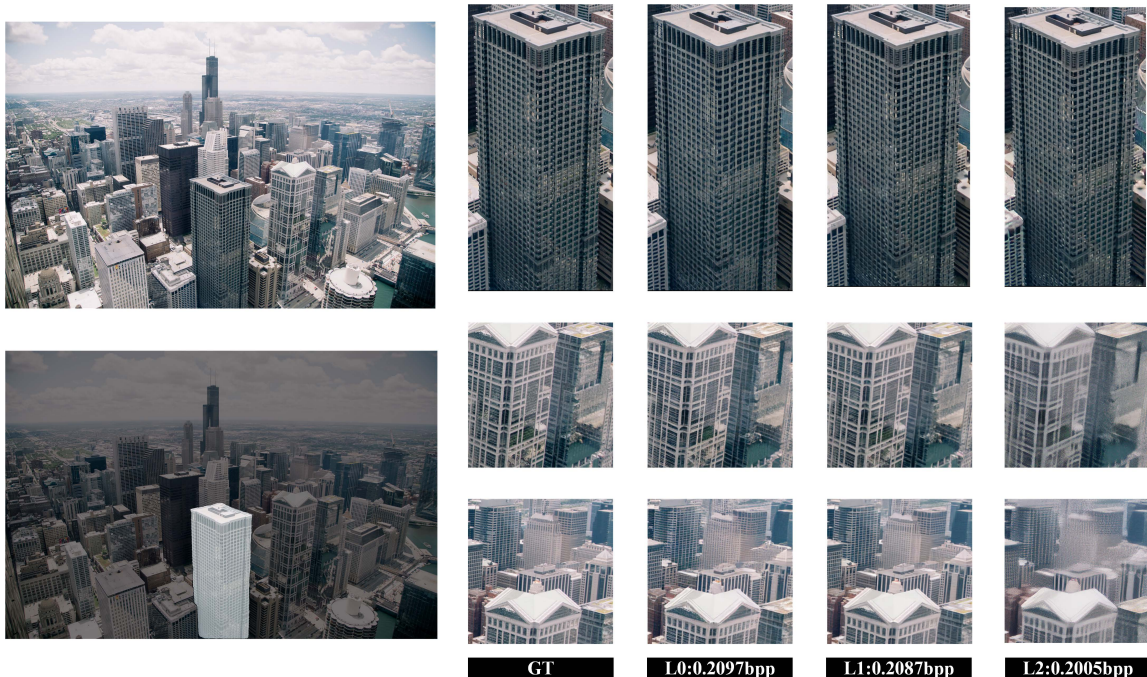


Fig. 4: Qualitative comparison of refining latent representations using different sets of hyperparameters for ROI-based loss.

D. Ablation Study

Our ablation studies aimed to assess the impact of different components in the proposed semantic ensemble loss. We trained models with varying losses at 0.15 bpp and evaluated their performance. The results, presented in Tab. I, indicate that omitting style loss, perceptual loss, and adversarial loss results in FIDs of 12.44, 13.32, and 13.85, respectively. These findings highlight the significance of each component in the semantic ensemble loss, particularly the non-binary adversarial loss, which proves to be the most influential.

IV. CONCLUSION

This study introduces a codec optimized for visual quality, leveraging semantic ensemble loss and latent

TABLE I: Ablation studies on different terms in semantic ensemble loss.

Methods	FID↓
Ours	11.88
w/o style loss	12.95
w/o perceptual loss	13.44
w/o non-binary adversarial loss	13.85

representation refinement. Our codec integrates semantic ensemble loss to enhance the model's ability to generate finer details. To achieve better performance and bit allocation, we employed SGA with learnable quantization for fine-tuning latent representations. Extensive experiments demonstrate that our method sets

a new benchmark in image compression, excelling in perceptual quality compared to prior works.

ACKNOWLEDGMENT

This work was supported in part by National Key Research and Development Program of China under Grant 2022YFF1202104, in part by National Natural Science Foundation of China under Grants 62301188, 92270116 and U23B2009, in part by China Postdoctoral Science Foundation under Grant 2022M710958, and in part by Heilongjiang Postdoctoral Science Foundation under Grant LBH-Z22156.

REFERENCES

- [1] E. Agustsson, M. Tschanen, F. Mentzer, R. Timofte, and L. Van Gool, "Generative Adversarial Networks for Extreme Learned Image Compression," in *2019 IEEE/CVF International Conference on Computer Vision (ICCV)*. Seoul, Korea (South): IEEE, Oct. 2019, pp. 221–231.
- [2] Y. Bai, X. Liu, K. Wang, X. Ji, X. Wu, and W. Gao, "Deep lossy plus residual coding for lossless and near-lossless image compression," *IEEE Transactions on Pattern Analysis and Machine Intelligence*, 2024.
- [3] Y. Bai, X. Liu, W. Zuo, Y. Wang, and X. Ji, "Learning scalable ∞ -constrained near-lossless image compression via joint lossy image and residual compression," in *Proceedings of the IEEE/CVF Conference on Computer Vision and Pattern Recognition*, 2021, pp. 11 946–11 955.
- [4] B. Bross, Y.-K. Wang, Y. Ye, S. Liu, J. Chen, G. J. Sullivan, and J.-R. Ohm, "Overview of the Versatile Video Coding (VVC) Standard and its Applications," *IEEE Transactions on Circuits and Systems for Video Technology*, vol. 31, no. 10, pp. 3736–3764, Oct. 2021.
- [5] K. Ding, K. Ma, S. Wang, and E. P. Simoncelli, "Image Quality Assessment: Unifying Structure and Texture Similarity," *IEEE Transactions on Pattern Analysis and Machine Intelligence*, pp. 1–1, 2020.
- [6] C. Gao, T. Xu, D. He, Y. Wang, and H. Qin, "Flexible Neural Image Compression via Code Editing," *Advances in Neural Information Processing Systems*, vol. 35, pp. 12 184–12 196, Dec. 2022.
- [7] S. Gao, Y. Shi, T. Guo, Z. Qiu, Y. Ge, Z. Cui, Y. Feng, J. Wang, and B. Bai, "Perceptual learned image compression with continuous rate adaptation," *4th Challenge on Learned Image Compression*, vol. 2, no. 3, 2021.
- [8] D. He, Z. Yang, W. Peng, R. Ma, H. Qin, and Y. Wang, "ELIC: Efficient Learned Image Compression with Unevenly Grouped Space-Channel Contextual Adaptive Coding," in *2022 IEEE/CVF Conference on Computer Vision and Pattern Recognition (CVPR)*. New Orleans, LA, USA: IEEE, Jun. 2022, pp. 5708–5717.
- [9] D. He, Z. Yang, H. Yu, T. Xu, J. Luo, Y. Chen, C. Gao, X. Shi, H. Qin, and Y. Wang, "PO-ELIC: Perception-Oriented Efficient Learned Image Coding," in *2022 IEEE/CVF Conference on Computer Vision and Pattern Recognition Workshops (CVPRW)*. New Orleans, LA, USA: IEEE, Jun. 2022, pp. 1763–1768.
- [10] M. Heusel, H. Ramsauer, T. Unterthiner, B. Nessler, and S. Hochreiter, "Gans trained by a two time-scale update rule converge to a local nash equilibrium," *Advances in neural information processing systems*, vol. 30, 2017.
- [11] A. Kirillov, E. Mintun, N. Ravi, H. Mao, C. Rolland, L. Gustafson, T. Xiao, S. Whitehead, A. C. Berg, W.-Y. Lo, P. Dollár, and R. Girshick, "Segment Anything," Apr. 2023.
- [12] I. Krasin, T. Duerig, N. Alldrin, A. Veit, S. Abu-El-Haija, S. Belongie, D. Cai, Z. Feng, V. Ferrari, and V. Gomes, *OpenImages: A Public Dataset for Large-Scale Multi-Label and Multi-Class Image Classification.*, Jan. 2016.
- [13] W.-S. Lai, J.-B. Huang, N. Ahuja, and M.-H. Yang, "Deep laplacian pyramid networks for fast and accurate super-resolution," in *Proceedings of the IEEE conference on computer vision and pattern recognition*, 2017, pp. 624–632.
- [14] D. Li, Y. Bai, K. Wang, J. Jiang, X. Liu, and W. Gao, "Grouped-mixer: An entropy model with group-wise token-mixers for learned image compression," *IEEE Transactions on Circuits and Systems for Video Technology*, 2024.
- [15] P. Liang, J. Jiang, X. Liu, and J. Ma, "Image deblurring by exploring in-depth properties of transformer," *IEEE Transactions on Neural Networks and Learning Systems*, 2024.
- [16] Y. Ma, Y. Zhai, C. Yang, J. Yang, R. Wang, J. Zhou, K. Li, Y. Chen, and R. Wang, "Variable Rate ROI Image Compression Optimized for Visual Quality," in *2021 IEEE/CVF Conference on Computer Vision and Pattern Recognition Workshops (CVPRW)*. Nashville, TN, USA: IEEE, Jun. 2021, pp. 1936–1940.
- [17] F. Mentzer, G. D. Toderici, M. Tschanen, and E. Agustsson, "High-fidelity generative image compression," *Advances in Neural Information Processing Systems*, vol. 33, pp. 11 913–11 924, 2020.
- [18] M. J. Muckley, A. El-Nouby, K. Ullrich, H. Jegou, and J. Verbeek, "Improving Statistical Fidelity for Neural Image Compression with Implicit Local Likelihood Models," in *Proceedings of the 40th International Conference on Machine Learning*. PMLR, Jul. 2023, pp. 25 426–25 443.
- [19] X. Pan, Y. Gao, Z. Guo, R. Feng, and Z. Chen, "Perceptual image compression with controllable region quality," ser. 5th Challenge on Learned Image Compression, 2022.
- [20] M. S. Sajjadi, B. Scholkopf, and M. Hirsch, "Enhancenet: Single image super-resolution through automated texture synthesis," in *Proceedings of the IEEE international conference on computer vision*, 2017, pp. 4491–4500.
- [21] J.D. Sutherland, M. Arbel, and A. Gretton, "Demystifying MMD GANs," in *International Conference for Learning Representations*, 2018, pp. 1–36.
- [22] K. Wang, Y. Bai, D. Li, D. Zhai, J. Jiang, and X. Liu, "Learning lossless compression for high bit-depth volumetric medical image," 2024. [Online]. Available: <https://arxiv.org/abs/2410.17814>
- [23] K. Wang, Y. Bai, D. Zhai, D. Li, J. Jiang, and X. Liu, "Learning lossless compression for high bit-depth medical imaging," in *2023 IEEE International Conference on Multimedia and Expo (ICME)*. IEEE, 2023, pp. 2549–2554.
- [24] Y. Yang, R. Bamler, and S. Mandt, "Improving Inference for Neural Image Compression," in *Advances in Neural Information Processing Systems*, vol. 33. Curran Associates, Inc., 2020, pp. 573–584.
- [25] R. Zhang, P. Isola, A. A. Efros, E. Shechtman, and O. Wang, "The unreasonable effectiveness of deep features as a perceptual metric," in *Proceedings of the IEEE Conference on Computer Vision and Pattern Recognition*, 2018, pp. 586–595.